

Supplementary information

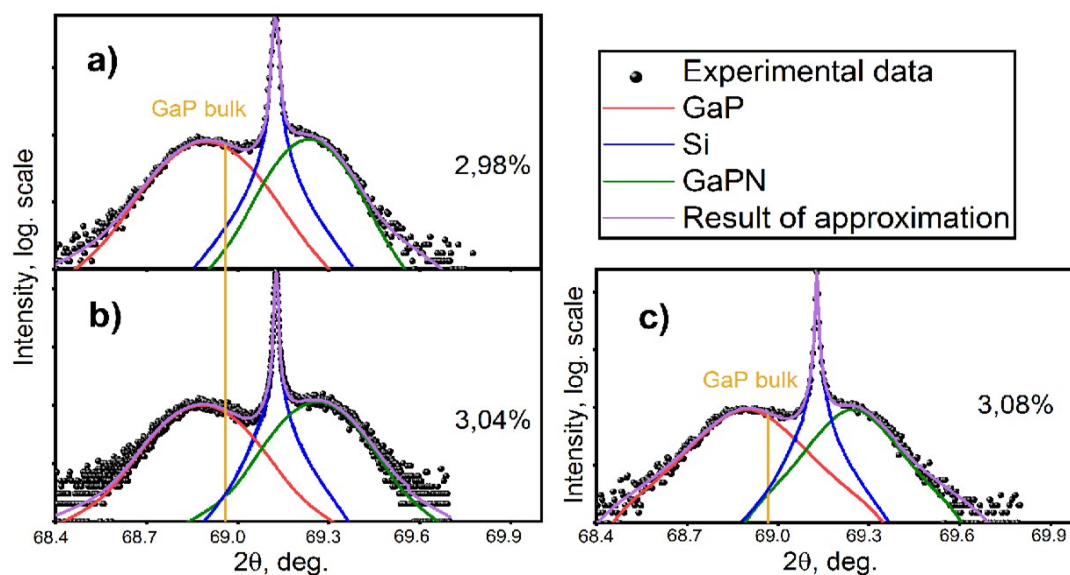


Fig. 1. Experimental Θ - 2Θ XRD scans of the studied samples (#2, #3 and #4) across the Si (004) symmetric Bragg reflection and theoretical fits approximated with pseudo-Voigt function corresponding to Si, GaP, $\text{GaP}_{1-x}\text{N}_x$.

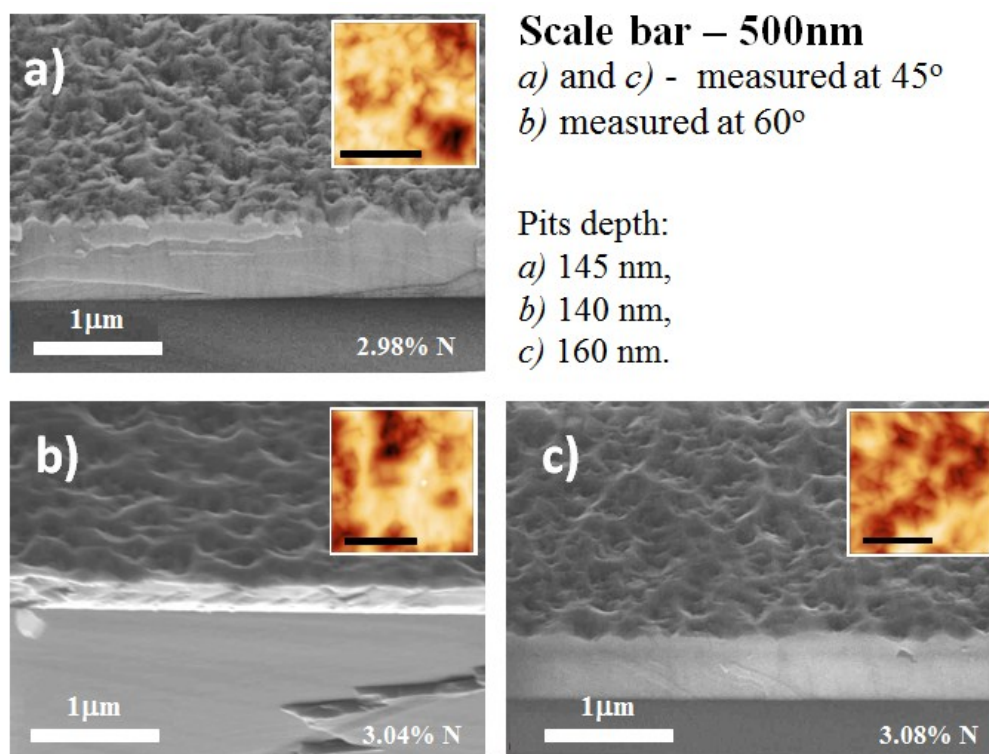


Fig. 2. SEM images and corresponding AFM scans (on insets, scale bar 500 nm) of (samples #2, #3, #4).

HRTEM

In Fig. 3 one can find cross-sectional HRTEM image of the surface area of sample #5 illustrating presence of the lamellar twinning. Twinning planes are marked by white arrows. Note that the surface roughness is correlated with the presence of twins.

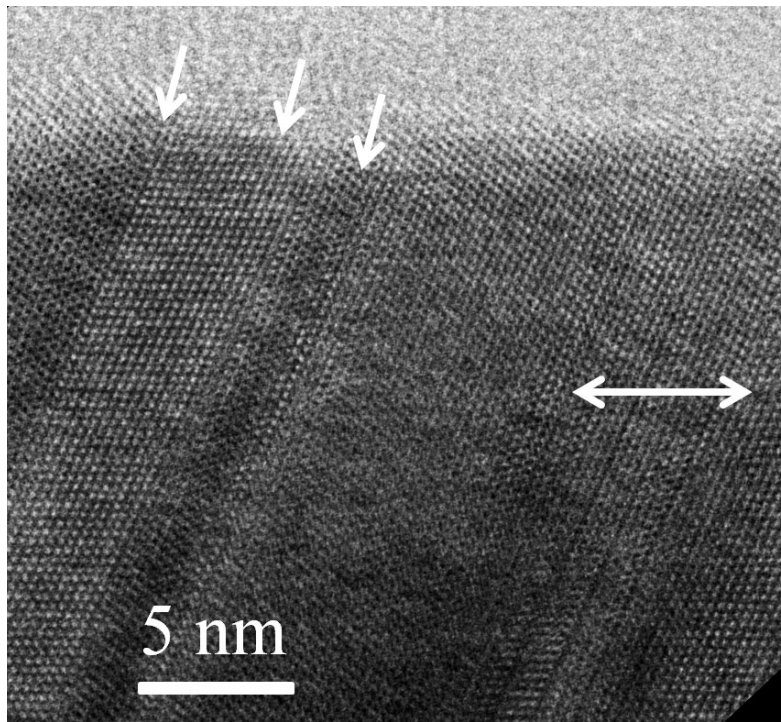


Fig. 3. HRTEM image of sample with 5.05% nitrogen content. White arrows indicate lamellar micro-twinning planes.

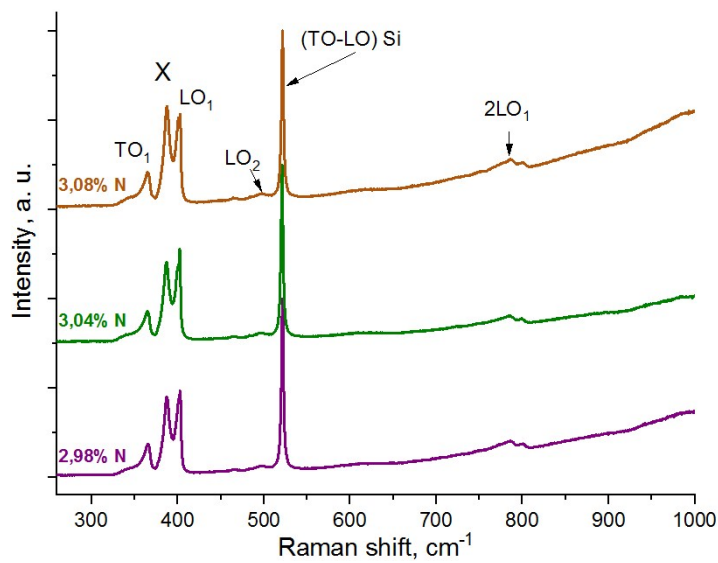


Fig. 4. RT RS spectra of the heterostructures with ~ 2.98 , 3.04 and 3.08% nitrogen content (samples #2, #3, #4).

RF plasma source characterization

In addition to the measurements of the nitrogen plasma optical emission intensity by a silicon photodetector we obtain information on its degree of ionization by a spectral analysis performed with SOLAR Laser Systems S100 spectrometer. Spectra in Fig.5 were obtained for a N_2 gas flow of 0.3 (red curve) and 1 (black curve) sccm at 450W of RF power. Analysis of the emission spectra was conducted according to the results of [1], [2]. One can note sharp lines in the near-UV and IR. The sharp near-UV lines can be attributed to the 1st negative system of N^{2+} ion transitions, while three sharpest and strongest emissions at about 745, 821 and 869 nm correspond to the atomic nitrogen. Broad emission bands in the range of 550-750 nm are attributed to the emission of vibrationally excited neutral N_2 molecules.

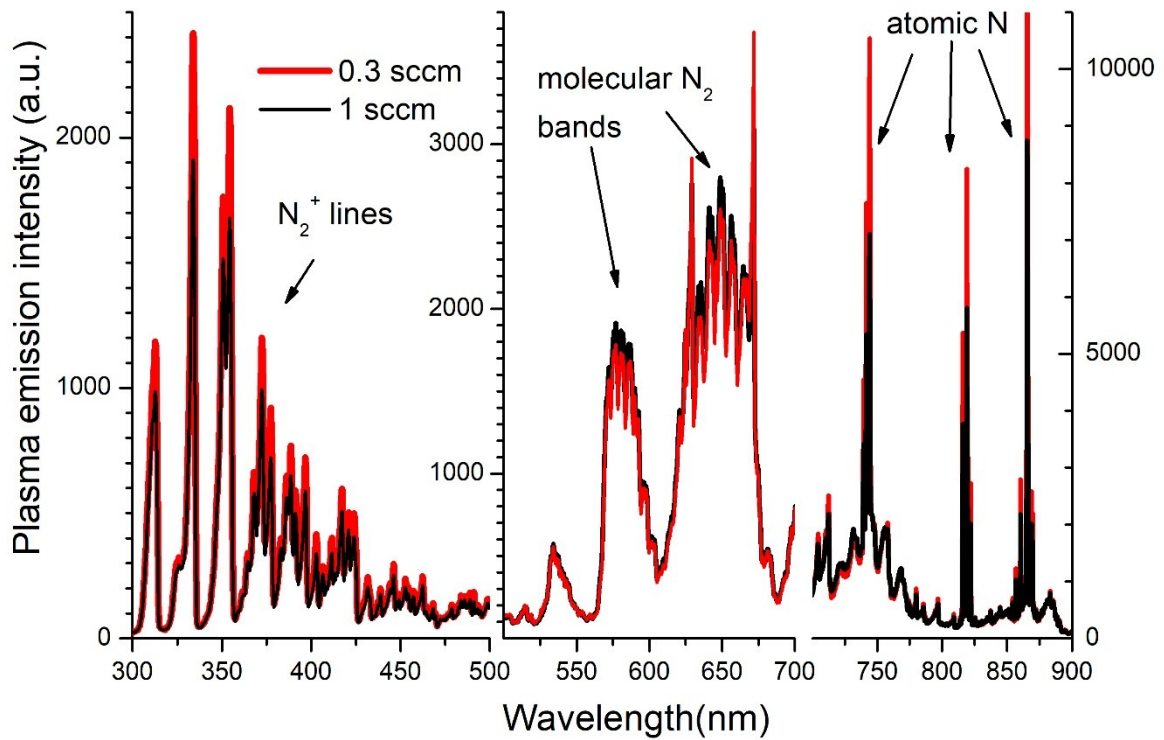


Fig. 5. Optical emission spectra of the nitrogen RF plasma cell obtained at 450W of RF power and 1 and 0.3 sccm of N_2 flow.

Intensity of the emission lines corresponding to atomic nitrogen are proportional to the RF power and reaches a maximum at a low mass flow rate of N_2 (less than ~ 0.3 sccm), and decreases with increasing mass flow rate. Similar to the atomic lines N_2^+ ion transitions are also appearing brighter at low N_2 fluxes. In contrast, intensity of neutral N_2 molecule emission bands increase with mass flow rate while the fraction of ionized species decreased, what is consistent with the results of [2]. Thus, we assume that active nitrogen flux generated at nitrogen flow of 1.1 sccm contain a smaller number of ionized species compare to 0.3sccm.

[1] M. A. Wistey, S. R. Bank, H. B. Yuen, H. Bae, and J. S. Harris, "Nitrogen plasma optimization for high-quality dilute nitrides," *J. Cryst. Growth*, vol. 278, no. 1–4, pp. 229–233, May 2005.

[2] H. Carrère, A. Arnoult, A. Ricard, X. Marie, T. Amand, and E. Bedel-Pereira, "Nitrogen-plasma study for plasma-assisted MBE growth of 1.3 μm laser diodes," *Solid. State. Electron.*, vol. 47, no. 3, pp. 419–423, Mar. 2003.

AFM analysis of the surface morphology

Statistical analysis of the sample morphology obtained by the AFM measurements is presented in the table below. Columns labeled as "max. hillock height" and "max. pit depth" indicate maximum and minimum height deviation from a mean surface level correspondingly.

Table 1. Statistical analysis of the surface morphology

Sample	N Content, %	RMS roughness, nm	max. hillock height, nm	max. pit depth, nm
#1	0	5.0	6.3	65.0
#2	2.98	19.8	47.1	99.4
#3	3.08	24.2	66.9	92.7
#4	3.04	22.6	54.8	85.1
#5	5.05	19.5	67.5	76.9

#6	3.07	21.9	51.0	81.9
#7	3.66	22.4	56.9	112.5

Figure 6 illustrates no direct correlation between nitrogen content and surface roughness.

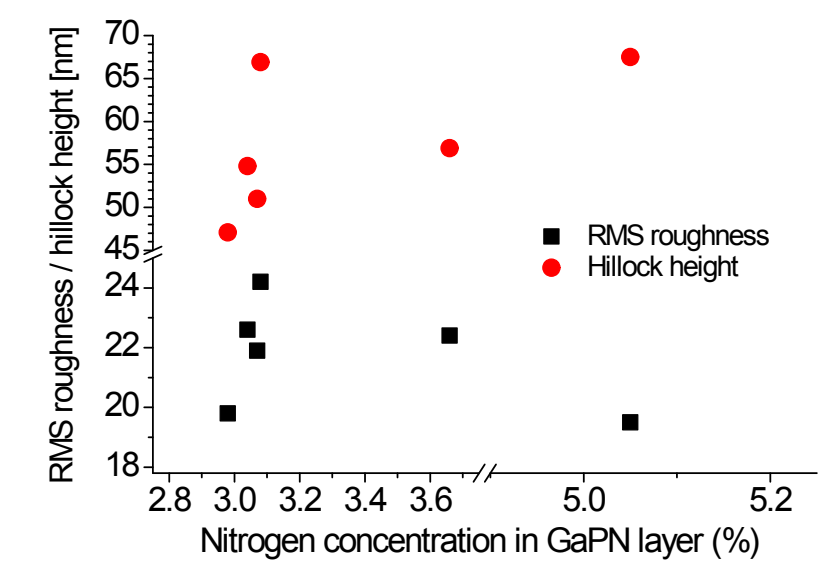


Fig. 6. Dependences of the sample roughness on nitrogen content.